A wave based condensation method for computing the acoustic efficiency of sound packages submitted to sliding or clamped lateral boundary conditions.

Q. Serra [1,2]**, M.N. Ichchou** [1]**, J-F. Deü** [2]
[1] Ecole Centrale de Lyon, Laboratoire de Tribologie et de Dynamique des Systèmes,
36 avenue Guy de Collongue, 69130 Ecully, France.
e-mail: **quentin.serra@ec-lyon.fr**

[2] Cnam Paris, Laboratoire de Mécanique des Structures et des Systèmes Couplés,
2 rue Conté, 75003 Paris, France.

Abstract
In this work, we propose a generalized impedance approach to model dissipative interfaces used in vibroacoustic systems, usually composed of poroelastic materials. This approach is based, like the classical impedance approach, on wave propagation. In the usual approach, the impedance is derived by Transfer Matrix Method (TMM) from the knowledge of the waves propagating in the thickness of a laterally infinite medium. Here, using Wave Finite Element Method (WFE), are predicted waves propagating in the thickness of the medium and taking into account the lateral boundaries. It is shown on several examples that these waves make possible to express the contribution of the dissipative layers on master parts, and thus to reduce the size of the global system. Compared to the usual impedance approach, the present method makes possible to use the exact value of the impedance coefficient, taking into account the effect of the lateral boundary conditions and of non-local effects on the response of the system.

1 Introduction

When dealing with the vibroacoustic response of systems involving vibrating structures, acoustic cavities and dissipative interfaces, the key point is the modelling of the dissipative interface without introducing too much computational complexity. Indeed, these dissipative interfaces are most often multilayer panels including poroelastic materials. The complex behaviour of such materials can be predicted by using Biot-Allard's theory, leading though to very large computational cost if the Finite Element Method (FEM) is used.

Several works deals with the reduction of the computational cost of the problem by using Component Mode Synthesis (CMS) [1, 2, 3]. The limit of the approach lies in the large number of modes needed in the case of complex geometries or in the high frequency range. Some others (e.g. [4, 5]) investigate the use of Padé approximants to reduce the number of frequency steps of the computation. However, the accuracy of the method is penalized by the choice of the evaluation frequencies. An adaptive algorithm can be used to find the optimal evaluation points. Finally the efficiency of the method is limited by the need to compute the response of the whole system at these points.

Typically, the common procedure consists in representing the interface by a constant coefficient, the wall impedance, typically measured or computed by the Transfer Matrix Method (TMM) [6]. This method is based on the representation of the movement as resulting from the contribution of propagating waves. It results in very small computational times and can be used for multilayer packages. This method can also

be combined with FEM to eliminate the unknowns associated to the interface [7], to simulate the acoustic response in the case of inhomogeneous dissipative panels, or to change the incidence angles depending on the position of the element. However, TMM assumes flat geometry and infinite lateral dimensions. By hypothesis, the method can not take into account effects of the boundary conditions, resulting from the interaction of outward going waves and reflected waves on the boundaries. Another set of transfer matrix methods is derived from the Floquet theory, using the hypothesis of periodicity. Among them, the Wave Finite Element Method (WFE) [9, 10, 11] makes possible to compute propagating waves in a complex cross-section unidirectional waveguide. This method makes possible to generalize the TMM by taking into account the lateral boundary conditions, and extends naturally to non locally reacting materials. This method has been intensively used in the last years in the case of elastic and viscoelastic layers [11, 12, 13, 14, 15, 16, 17]. It makes possible to compute both dispersion curves and section modes. It can be used either to analyse energy transfer mechanisms between waves or to predict the response of a structure by projecting the unknowns on the basis of propagative waves.

We propose here an hybrid WFE-FEM method making possible to simulate at a reduced cost and in a large frequency range the acoustic performance of a sound package. This technique is based on the derivation of an additional dynamic stiffness matrix representing for the contribution of the interface on the master domains. Such an approach has been used recently in [8] to couple FEM and TMM within Green function formalism, making possible to extend the classical localized impedance to non-localized configurations by a semi-analytical algorithm. In the present work, the correction matrix is expressed numerically as a function of the wave modes predicted by WFE. These waves are compatible with the lateral boundary conditions applied on the dissipative layer, so the correction matrix contains all of the information on the effect of lateral boundary conditions.

The outline of the paper is the following. First, impedance approach is briefly recalled, then the calculation of wave modes by WFE is presented. Thirdly the expression of the additional matrix representing for the effect of the interface on the master system is derived as a function of the wave modes, in two cases: (i) an absorption problem, (ii) the problem of transmission of sound through a two-layer poroelastic medium submitted to sliding or clamped boundary conditions. Finally, several remarks on the computational cost are presented.

2 Condensation on the interfaces of a poroelastic-acoustic system

We consider a system composed of a rigid acoustic cavity, covered partially by a poroelastic single layer on a flat rigid wall (see Fig. 1). All of the other walls are rigid. No structural load excites the poroelastic domain. The acoustic domain is written Ω_A, the acoustic pressure is p_{a}. The poroelastic domain is written Ω_{P} and is modelled using the ($\mathbf{u}^{\mathrm{s}}$,$\mathbf{u}^{\mathrm{t}}$) formulation [18], denoting respectively the solid phase displacement and the total displacement. The poroelastic/acoustic interface is written Γ and $\mathbf{n}_{\mathrm{A}}$ (resp. $\mathbf{n}_{\mathrm{P}}$) is the normal vector on Γ, pointing outward the domain Ω_A (resp. Ω_{P}). The variational formulation of the system can be expressed in the frequency domain ($\exp(\mathrm{i}\omega t)$) by:

- for the acoustic cavity:

$$\begin{gathered}\text{find } p_{\mathrm{a}} \text{ such as for all } \delta p_{\mathrm{a}} : \\ \int_{\Omega_{\mathrm{A}}} \left(\tfrac{1}{\rho_0 \omega^2} \nabla p_{\mathrm{a}} \nabla \delta p_{\mathrm{a}} - \tfrac{1}{\rho_0 c_0^2} p_{\mathrm{a}} \delta p_{\mathrm{a}} \right) \mathrm{d}\Omega_{\mathrm{A}} = \int_{\Gamma} \mathbf{u}^{\mathrm{t}} \cdot \mathbf{n}_{\mathrm{A}} \delta p_{\mathrm{a}} \mathrm{d}\Gamma,\end{gathered} \tag{1}$$

- for the poroelastic domain:

$$\begin{gathered}\text{find } \mathbf{u}^{\mathrm{s}} \text{ and } \mathbf{u}^{\mathrm{t}} \text{ such as for all } \delta\mathbf{u}^{\mathrm{s}} \text{ and } \delta\mathbf{u}^{\mathrm{t}} : \\ \int_{\Omega_{\mathrm{P}}} \left(\hat{\boldsymbol{\sigma}}^{\mathbf{s}} : \boldsymbol{\varepsilon}(\delta\mathbf{u}^{\mathrm{s}}) - \omega^2 \tilde{\rho}_{\mathrm{s}} \mathbf{u}^{\mathrm{s}} \cdot \delta\mathbf{u}^{\mathrm{s}} - \omega^2 \tilde{\gamma} \tilde{\rho}_{\mathrm{eq}} \mathbf{u}^{\mathrm{t}} \cdot \delta\mathbf{u}^{\mathrm{s}} \right) \mathrm{d}\Omega_{\mathrm{P}} \\ + \int_{\Omega_{\mathrm{P}}} \left(-p\mathbf{I} : \boldsymbol{\varepsilon}(\delta\mathbf{u}^{\mathrm{t}}) - \omega^2 \tilde{\gamma} \tilde{\rho}_{\mathrm{eq}} \mathbf{u}^{\mathrm{s}} \cdot \delta\mathbf{u}^{\mathrm{t}} - \omega^2 \tilde{\rho}_{\mathrm{eq}} \mathbf{u}^{\mathrm{t}} \cdot \delta\mathbf{u}^{\mathrm{t}} \right) \mathrm{d}\Omega_{\mathrm{P}} = \int_{\Gamma} -p_{\mathrm{a}} \mathbf{n}_{\mathrm{P}} \cdot \delta\mathbf{u}^{\mathrm{t}} \mathrm{d}\Gamma,\end{gathered} \tag{2}$$

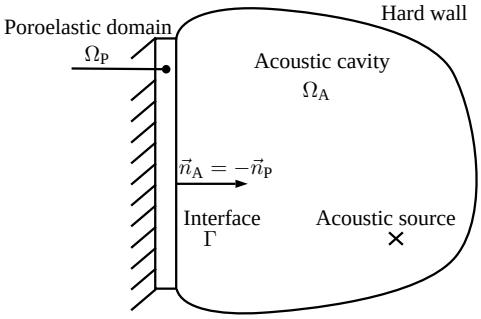

Figure 1: Description of a poroacoustic problem.

where ρ_0 and c_0 are respectively the density and the sound velocity of the acoustic air, where the coefficients $\tilde{\rho}_{\rm eq}$ and $\tilde{\rho}_{\rm s}$ are equivalent densities characterizing respectively the fluid when the skeleton is motionless and the skeleton, where $\tilde{\gamma}$ is a coupling coefficient, where $\varepsilon(\mathbf{u}) = \frac{1}{2}\left(\nabla\mathbf{u} + \nabla^T\mathbf{u}\right)$ is the strain tensor associated to the displacement field $\mathbf{u}$ and where p is the pore pressure. It is given as a function of the total displacement and of the bulk modulus of the poroelastic material $\tilde{K}_{\rm eq}$ by:

$$p = -\tilde{K}_{\rm eq}\nabla\cdot\mathbf{u}^{\rm t}. \tag{3}$$

Finally $\hat{\boldsymbol{\sigma}}^{\rm s}$ is the stress tensor of the *in-vacuo* skeleton, and does not depend of the pore pressure. Expression of all of the parameters depending on frequency can be found in [6, 18].

After discretization by Finite Elements, the dynamic equilibrium is obtained under the form:

$$\begin{bmatrix}\mathbf{D}_{\rm AA}(\omega) & \mathbf{D}_{\rm AP}\\ \mathbf{D}_{\rm AP}^T & \mathbf{D}_{\rm PP}(\omega)\end{bmatrix}\begin{pmatrix}\mathbf{p}_{\rm A}(\omega)\\ \mathbf{q}_{\rm P}(\omega)\end{pmatrix} = \begin{pmatrix}\mathbf{F}_{\rm A}(\omega)\\ \mathbf{0}\end{pmatrix} \tag{4}$$

where $\mathbf{p}_{\rm A}$ and $\mathbf{q}_{\rm P}$ are respectively the vectors of the nodal pressures in the cavity, and the vector of nodal unknowns in the poroelastic domain, where the blocs $\mathbf{D}_{\rm ii}$ for i=A,P are the dynamic stiffness matrices of the acoustic and the poroelastic domain, and where $\mathbf{D}_{\rm AP}$ is the coupling matrix. The problem has $n_{\rm A}$ degrees of freedom (dofs) associated to the acoustic domain and $n_{\rm P}$ dofs associated to the poroelastic domain.

If this approach can be easily implemented in a Finite Element program, it is limited by the numerical cost. The wavelengths travelling in the poroelastic medium are very short, and poroelastic elements are known to have a slow convergence rate. This means that the poroelastic domain have to be meshed very finely to provide accurate results, leading to a large number of nodes. Furthermore, with this formulation, 6 dofs per node are used. It results so in a problem involving a large number of dofs. The total problem may involve quite as many dofs for the poroelastic domain than for the acoustic domain, *i.e.* $n_{\rm A} \approx n_{\rm P}$, so that adding a dissipative interface to an acoustic rigid cavity increases considerably the computational cost. The number of unknowns per node can be reduced up to one dof per node by choosing an equivalent fluid model to represent the poroelastic material, but this approach can not be used for all kinds of materials. Nevertheless, the procedure presented here can easily be applied to the case of equivalent fluid models.

To predict the response of complex multilayer panels applied on large areas, these approaches lead to huge computation times, so that they are not used generally. Indeed, in this case, the poroelastic are modelled in most cases by an equivalent localized impedance, so that no unknown is used for the poroelastic domain.

2.1 Impedance approach

The impedance approach consists in the replacement of the three-dimensional modelling of the dissipative layers by a frequency dependent parameter. The idea behind the method is that if the load applied on the acoustical domain is known exactly, there is no need to solve for the dynamic response of the panel. First,

the work of the normal displacement of the dissipative interface on the acoustic cavity is written as a function of the acoustic pressure unknowns:

$$\int_\Gamma \mathbf{u}^{\mathrm{t}} \cdot \mathbf{n}_{\mathrm{A}} \delta p_{\mathrm{a}} \mathrm{d}\Gamma \approx {\mathbf{p}_{\mathrm{a}}}^T \mathbf{D}_{\mathrm{corr}} \mathbf{p}_{\mathrm{a}}. \tag{5}$$

The question is thus how to estimate the correction matrix $\mathbf{D}_{\mathrm{corr}}$. Knowing the localized impedance, defined by the ratio of the pressure by the normal velocity to the acoustic interface:

$$Z_{\mathrm{s}}(\omega) = \frac{p_{\mathrm{a}}(\omega)}{\mathrm{i}\omega \mathbf{u}^{\mathrm{t}} \cdot \mathbf{n}_{\mathrm{A}}} \tag{6}$$

the relation in (5) becomes:

$$\int_\Gamma \mathbf{u}^{\mathrm{t}} \cdot \mathbf{n}_{\mathrm{A}} \delta p_{\mathrm{a}} \mathrm{d}\Gamma = \int_\Gamma \frac{1}{\mathrm{i}\omega Z_{\mathrm{s}}(\omega)} p_{\mathrm{a}} \delta p_{\mathrm{a}} \mathrm{d}\Gamma. \tag{7}$$

If the interface is homogeneous in the section, it is reasonable to assume that the impedance is constant on the interface, so that the equations of the acoustic domain become:

$$\left(\mathbf{D}_{\mathrm{AA}}(\omega) - \mathbf{D}_{\mathrm{corr}}(\omega)\right) \mathbf{p}_{\mathrm{A}}(\omega) = \mathbf{F}_{\mathrm{a}}(\omega) \tag{8}$$

where the correction matrix $\mathbf{D}_{\mathrm{corr}}$ is:

$$\mathbf{D}_{\mathrm{corr}}(\omega) = \frac{1}{\mathrm{i}\omega Z_{\mathrm{s}}(\omega)} \mathbf{C} \tag{9}$$

and where the matrix $\mathbf{C}$ is such that:

$$\int_\Gamma p_{\mathrm{a}} \delta p_{\mathrm{a}} \mathrm{d}\Gamma \approx {\mathbf{p}_{\mathrm{a}}}^T \mathbf{C} \mathbf{p}_{\mathrm{a}}. \tag{10}$$

No unknown is associated to the poroelastic domain, so the size of the problem is only n_{A}. Computation time is slightly larger than for the problem without interface, because the problem involves complex matrices and is non linear in frequency, but is still very small. In particular, the method can be used for any type of multilayer packages since the impedance value of such package can be derived from TMM.

The difficulty of the approach lies in the estimation of the value of the impedance coefficient. Indeed, its value depends of the incidence angle and so of the excitation as well as on the boundary conditions. Classically is used the impedance coefficient measured in impedance tube or computed by TMM at normal incidence. Recently, Jeong and Brunskog [19] showed that for the absorption problem and locally reacting materials, the best incidence angle to represent a diffuse field is around 55°. Finally, it should be remarked that TMM is only valid for infinite geometries. If some boundary conditions are applied on the lateral faces of the package, reflection of waves at these boundaries may lead to non uniform impedance values, so that the value predicted by TMM may not reflect the real behaviour of the material. These effects may be neglected in most cases, when dimensions of the system are much larger than the wavelengths, but they may occur when small dimensions are considered.

In the two following sections, we show that for flat geometries, the procedure used here can be adapted to take into account lateral boundary conditions. A transfer matrix relating each section can be derived from Finite Elements matrices of a substructure of the poroelastic domain. This makes possible to derive the propagation constants and the section wave modes of the poroelastic sample. These modes can be used to express the correction matrix exactly, allowing to take into account boundary effects and non-localized effects.

2.2 Computation of propagatives modes

We consider a block of poroelastic medium, of arbitrary cross-section, and of thickness L_{P}. The system coordinates are written (x, y, z), where the thickness direction is z. It is possible to predict the waves

propagating in the medium, in the direction of the thickness, by using Floquet theory. Indeed, characteristics of the waves do not depend on the length of propagation. The medium being homogeneous, the material properties are constant in the thickness direction. It is possible to model only a substructure of length $d \ll L_{\mathrm{P}}$, for which the equations of the dynamic obtained by Finite Elements are:

$$\mathbf{D}(\omega)\mathbf{q}_{\mathrm{P}}(\omega) = \mathbf{F}_{\mathrm{P}}(\omega). \tag{11}$$

If only on element is used to mesh the thickness of the substructure, the vector of the nodal unknowns $\mathbf{q}_{\mathrm{P}}$ and of the nodal loads $\mathbf{F}_{\mathrm{P}}$ can be partitioned between the nodes present in the left section (1) $z = 0$ and the right section (2) $z = d$ under the form:

$$\begin{bmatrix} \mathbf{D}_{11} & \mathbf{D}_{12} \\ \mathbf{D}_{21} & \mathbf{D}_{22} \end{bmatrix} \begin{pmatrix} \mathbf{q}_{\mathrm{P}1} \\ \mathbf{q}_{\mathrm{P}2} \end{pmatrix} = \begin{pmatrix} \mathbf{F}_{\mathrm{P}1} \\ \mathbf{F}_{\mathrm{P}2} \end{pmatrix} \tag{12}$$

so that a transfer matrix relating nodal unknowns and the nodal loads between the two sections can be defined:

$$\mathbf{T} \begin{pmatrix} \mathbf{q}_{\mathrm{P}1} \\ -\mathbf{F}_{\mathrm{P}1} \end{pmatrix} = \begin{pmatrix} \mathbf{q}_{\mathrm{P}2} \\ \mathbf{F}_{\mathrm{P}2} \end{pmatrix} \tag{13}$$

with:

$$\mathbf{T} = \begin{bmatrix} -\mathbf{D}_{12}^{-1}\mathbf{D}_{11} & -\mathbf{D}_{12}^{-1} \\ \mathbf{D}_{21} - \mathbf{D}_{22}\mathbf{D}_{12}^{-1}\mathbf{D}_{11} & -\mathbf{D}_{22}\mathbf{D}_{12}^{-1} \end{bmatrix}. \tag{14}$$

Wave modes are the eigen modes of the transfer matrix $\mathbf{T}$:

$$\mathbf{T} = \mathbf{\Phi}\mathbf{\Lambda}\mathbf{\Phi}^{-1} \tag{15}$$

where $\mathbf{\Phi}$ is the matrix of the eigenvectors and $\mathbf{\Lambda} = (\mathrm{diag}(\lambda_i))_i$ is the matrix of the eigenvalues, called propagation constants. Each of the propagation constants is related to a wavenumber propagating in the direction z and to the length of the substructure:

$$\lambda_i = \exp(-\mathrm{i}k_z^i d). \tag{16}$$

Among the waves, half are such as $|\lambda_i| =< 1$. These waves propagate in the direction $+\mathbf{z}$ and are called progressive waves. The others propagate in the direction $-\mathbf{z}$.

When homogeneous Dirichlet boundary conditions are applied on lateral faces, such as sliding or clamped boundary conditions, the vector of unknowns $\mathbf{q}_{\mathrm{P}}$ can be partitioned into:

$$\mathbf{q}_{\mathrm{P}} = \left\langle \mathbf{q}_{\mathrm{P}r}^T, \mathbf{0}^T \right\rangle^T = \mathbf{R}\mathbf{q}_{\mathrm{P}r}. \tag{17}$$

The same procedure as previously can be followed, by replacing the dynamic stiffness matrix of the unconstrained substructure $\mathbf{D}$ by the constrained matrix $\mathbf{D}_c = \mathbf{R}^T\mathbf{D}\mathbf{R}$. The transfer matrix $\mathbf{T}_c$ obtained makes possible to define the modes of the non-constrained structure by $\mathbf{T}_c = \mathbf{\Phi}_c\mathbf{\Lambda}_c\mathbf{\Phi}_c^{-1}$. Finally, the mode shapes of the propagating modes in the structure are defined by:

$$\mathbf{\Phi} = \mathbf{R}\mathbf{\Phi}_c \tag{18}$$

and the waves propagate with the propagation constants $\mathbf{\Lambda}_c$.

For numerical reasons, the eigen modes are in fact not directly computed from the knowledge of the transfer matrix $\mathbf{T}$. Indeed, the inversion of the block $\mathbf{D}_{12}$ (Eq. (14)) may lead to large numerical errors. Here have been used the approach developed in [9].

This method can be used with any model and is valid either with displacement-displacement formulations, displacement-pressure formulations or equivalent fluid models. The difference between these possible choices lies in the conditioning of the matrices and appears when considering the expression of the forced response of the poroelastic sample to an arbitrary excitation. In the following section we consider the $(\mathbf{u}^{\mathrm{s}}, \mathbf{u}^{\mathrm{t}})$ formulation.

2.3 Condensation procedure

The aim of this section is to show how to compute the value of the correction matrix $\mathbf{D}_{\text{corr}}$ from the knowledge of the propagative modes.

2.3.1 Absorption problem

In this part, the condensation procedure is presented in the case of an absorption problem. The poroelastic sample is prescribed to an arbitrary pressure field $p_{\text{a}\Gamma}$ on $z = L_{\text{P}}$ and is clamped on the face $z = 0$.

In the present case, the boundary conditions are:

$$\begin{array}{c} \mathbf{F}_{\text{P}}(z = L_{\text{P}}) = \mathbf{F}_{A\to P} \\ \mathbf{q}_{\text{P}}(z = 0) = \mathbf{0} \end{array} \tag{19}$$

where the load exerted by the external pressure field $p_{\text{a}\Gamma}$ is written $\mathbf{F}_{A\to P}$ and is such as:

$$\int_{\Gamma} -p_{\text{a}\Gamma}\mathbf{n}_{\text{P}} \cdot \delta\mathbf{u}^{\text{t}}\text{d}\Gamma \approx \delta\mathbf{u}^{\text{t}^T}\mathbf{F}_{A\to P}. \tag{20}$$

Finally, the vector of external load acting on the poroelastic domain is:

$$\mathbf{F}_{A\to P} = -\mathbf{D}_{\text{AP}}^T\mathbf{p}_{\text{A}}. \tag{21}$$

The displacements and loads at the two sections are expressed as a combination of the propagative modes:

$$\begin{array}{c} \mathbf{\Phi}_q^+\mathbf{Q}^+(0) + \mathbf{\Phi}_q^-\mathbf{Q}^-(0) = \mathbf{0} \\ \mathbf{\Phi}_F^+\mathbf{Q}^+(L_{\text{P}}) + \mathbf{\Phi}_F^-\mathbf{Q}^-(L_{\text{P}}) = -\mathbf{D}_{\text{AP}}^T\mathbf{p}_{\text{A}} \end{array} \tag{22}$$

so that the amplitudes in the section $z = L_{\text{P}}$ are given by:

$$\begin{pmatrix} \mathbf{Q}^+(L_{\text{P}}) \\ \mathbf{Q}^-(L_{\text{P}}) \end{pmatrix} = \underbrace{\begin{bmatrix} \boldsymbol{\mu} & \mathbf{0} \\ \mathbf{0} & \mathbf{I} \end{bmatrix}}_{\mathbf{I}_L} \underbrace{\begin{bmatrix} \mathbf{I} & (\mathbf{\Phi}_q^+)^{-1}\mathbf{\Phi}_q^-\boldsymbol{\mu} \\ (\mathbf{\Phi}_F^-)^{-1}\mathbf{\Phi}_F^-\boldsymbol{\mu} & \mathbf{I} \end{bmatrix}^{-1}}_{\mathbf{B}^{-1}} \underbrace{\begin{pmatrix} \mathbf{0} \\ (\mathbf{\Phi}_F^-)^{-1}\mathbf{D}_{\text{AP}}^T\mathbf{p}_{\text{A}} \end{pmatrix}}_{\mathbf{F}_{\text{imp}}} \tag{23}$$

where the modes shapes $\mathbf{\Phi}$ are partitioned onto their displacements components $\mathbf{\Phi}_q$ and their load components $\mathbf{\Phi}_F$ and are separated in an equal set of progressive (+) and recessive (-) waves such as:

$$|\lambda_i^+| <= 1 \text{ and } |\lambda_i^-| >= 1. \tag{24}$$

The diagonal matrix $\boldsymbol{\mu}$ is defined by:

$$\boldsymbol{\mu} = (\text{diag}(\mu_i))_i \text{ with } \mu_i = (\lambda_i^+)^{L_{\text{P}}/d}. \tag{25}$$

The step of pre-multiplication by inverse matrices $(\mathbf{\Phi}_q^+)^{-1}$ and $(\mathbf{\Phi}_F^-)^{-1}$ and multiplication by $\boldsymbol{\mu}$ makes possible to normalize efficiently the matrix $\mathbf{B}$ and thus to reduce numerical errors during the resolution of the problem [20]. Furthermore, it can be observed that no exponentially growing term is used ($\|\mu\| < 1$), so the method is stable.

Now, referring to Eq. (1) and Eq. (4), it can be seen that only the poroelastic degrees of freedom present at the poroelastic interface are needed. Thus the fluid dynamic equilibrium can be written:

$$\mathbf{D}_{\text{AA}}\mathbf{p}_{\text{A}}(\omega) + \mathbf{D}_{\text{AP}}^*\mathbf{q}_{\text{P}|\Gamma}(\omega) = \mathbf{F}_{\text{A}}(\omega) \tag{26}$$

where $\mathbf{D}^*_{\mathrm{AP}}$ is the restriction of the coupling matrix $\mathbf{D}_{\mathrm{AP}}$ to the poroelastic degrees of freedom $\mathbf{q}_{\mathrm{P}|\Gamma}$ at the poroelastic-acoustic interface Γ. This vector is also the value of the degrees of freedom present on the section $z = L_{\mathrm{P}}$, which means:

$$\mathbf{q}_{\mathrm{P}|\Gamma} = \mathbf{q}_{\mathrm{P}\,z=L_{\mathrm{P}}} = \left[\mathbf{\Phi}^+_q, \mathbf{\Phi}^-_q\right] \begin{pmatrix} \mathbf{Q}^+(L_{\mathrm{P}}) \\ \mathbf{Q}^-(L_{\mathrm{P}}) \end{pmatrix}. \tag{27}$$

It can be observed that the vector $\mathbf{F}_{\mathrm{imp}}$ can be written as a function of the vector of the nodal pressures of the acoustic cavity:

$$\mathbf{F}_{\mathrm{imp}} = \begin{pmatrix} \mathbf{0} \\ (\mathbf{\Phi}^-_F)^{-1}\mathbf{D}^T_{\mathrm{AP}}\mathbf{p}_{\mathrm{A}} \end{pmatrix} = \mathbf{C}\mathbf{p}_{\mathrm{A}} \tag{28}$$

so that finally the dynamic equilibrium of the acoustic cavity can be written under the form:

$$\left(\mathbf{D}_{\mathrm{AA}} + \mathbf{D}_{\mathrm{corr}}\right)\mathbf{p}_{\mathrm{A}}(\omega) = \mathbf{F}_{\mathrm{A}}(\omega) \tag{29}$$

with

$$\mathbf{D}_{\mathrm{corr}} = \mathbf{D}^*_{\mathrm{AP}}\left[\mathbf{\Phi}^+_q, \mathbf{\Phi}^-_q\right]\mathbf{I}_L\mathbf{B}^{-1}\mathbf{C}. \tag{30}$$

2.3.2 Transmission problem

This work can also be done to express the correction matrix in a transmission problem, when two arbitrary pressure fields are applied on the two extremities of the sample. The acoustic domains are partitioned into domain 1 (excitation room) and domain 2 (reception room). The global system of equations can be written:

$$\begin{pmatrix} \mathbf{D}_{11} & \mathbf{0} & \mathbf{D}_{1\mathrm{P}} \\ \mathbf{0} & \mathbf{D}_{22} & \mathbf{D}_{2\mathrm{P}} \\ \mathbf{D}_{\mathrm{P}1} & \mathbf{D}_{\mathrm{P}2} & \mathbf{D}_{\mathrm{PP}} \end{pmatrix} \begin{pmatrix} \mathbf{p}_{\mathrm{A}1} \\ \mathbf{p}_{\mathrm{A}2} \\ \mathbf{q}_{\mathrm{P}} \end{pmatrix}(\omega) = \begin{pmatrix} \mathbf{F}_1 \\ \mathbf{F}_2 \\ \mathbf{0} \end{pmatrix}(\omega) \tag{31}$$

where the matrices $\mathbf{D}_{11}$ and $\mathbf{D}_{22}$ are the matrices of the acoustic domains 1 and 2 respectively, where $\mathbf{D}_{PP}$ is the dynamic stiffness matrix of the poroelastic sample. The anti-diagonal blocs $\mathbf{D}_{i\mathbf{P}}$ for $i \in \{1, 2\}$ are coupling matrices, and are such that $\mathbf{D}_{\mathbf{P}i} = \mathbf{D}_{i\mathbf{P}}{}^T$. It can be shown that the same form as previously is obtained:

$$\left[\begin{pmatrix} \mathbf{D}_{11} & \mathbf{0} \\ \mathbf{0} & \mathbf{D}_{22} \end{pmatrix} + \mathbf{D}_{\mathrm{corr}}\right] \begin{pmatrix} \mathbf{p}_{\mathrm{A}1} \\ \mathbf{p}_{\mathrm{A}2} \end{pmatrix}(\omega) = \begin{pmatrix} \mathbf{F}_1 \\ \mathbf{F}_2 \end{pmatrix}(\omega) \tag{32}$$

where the correction matrix is given by:

$$\mathbf{D}_{\mathrm{corr}} = \begin{bmatrix} \mathbf{D}^*_{1\mathrm{P}}\left[\mathbf{\Phi}^+_q, \mathbf{\Phi}^-_q\right]\mathbf{I}_1\mathbf{B}^{-1}\mathbf{C} \\ \mathbf{D}^*_{2\mathrm{P}}\left[\mathbf{\Phi}^+_q, \mathbf{\Phi}^-_q\right]\mathbf{I}_2\mathbf{B}^{-1}\mathbf{C} \end{bmatrix}. \tag{33}$$

The matrices $\mathbf{D}^*_{\mathrm{iP}}$ for $i \in \{1, 2\}$ denote repectively the part of the coupling matrices $\mathbf{D}_{\mathrm{iP}}$ relative to the poroelastic degrees of freedom on the interface between the domain i and the poroelastic domain. The matrix $\mathbf{C}$ makes possible to compute the load exerted on each wave due to an pressure loading on each side of the porous domain. It is given by:

$$\mathbf{C} = \begin{bmatrix} \left(\mathbf{\Phi}^+_F\right)^{-1}\mathbf{D}_{\mathrm{P}1} & \mathbf{0} \\ \mathbf{0} & -\left(\mathbf{\Phi}^-_F\right)^{-1}\mathbf{D}_{\mathrm{P}2} \end{bmatrix}. \tag{34}$$

The matrix $\mathbf{B}$ can be computed by:

$$\mathbf{B} = \begin{bmatrix} \mathbf{I} & (\mathbf{\Phi}^+_F)^{-1}\mathbf{\Phi}^-_F\boldsymbol{\mu} \\ (\mathbf{\Phi}^-_F)^{-1}\mathbf{\Phi}^+_F\boldsymbol{\mu} & \mathbf{I} \end{bmatrix} \tag{35}$$

where $\boldsymbol{\mu} = \mathrm{diag}(\mu_i)$ with $\mu_i = (\lambda^+_i)^{L_{\mathrm{P}}/d}$.

Finally the matrices $\mathbf{I}_1$ and $\mathbf{I}_2$ are given by:

$$\mathbf{I}_1 = \begin{bmatrix} \mathbf{I} & \mathbf{0} \\ \mathbf{0} & \boldsymbol{\mu} \end{bmatrix}, \quad \mathbf{I}_2 = \begin{bmatrix} \boldsymbol{\mu} & \mathbf{0} \\ \mathbf{0} & \mathbf{I} \end{bmatrix}. \tag{36}$$

2.3.3 Case of multilayers

In the case of composite materials, where different materials are used in the section but their arrangement is constant in the thickness of the sample (e.g. double porosity materials), the previous approach is still valid. However, when several layers of different materials are used in the thickness direction, the approach previously developed has to be modified to add continuity equations at the interfaces.

First, the wave modes of each of the layers are evaluated separately. Then, continuity of the displacements is assessed at each interface i separating the layer $i-1$ and the layer i. At a poroelastic/poroelastic interface, the use of $(\mathbf{u}^{\mathrm{s}}, \mathbf{u}^{\mathrm{t}})$ formulation within the Johnson-Champoux-Allard [6] approximation results in the continuity of the pressure and of the invacuo stress tensor, as well as of the solid displacement and the normal total displacement but also in the discontinuity of the transverse total displacements. The continuity of the continuous part c of the displacements is written by:

$$\left(\boldsymbol{\Phi}_{q_{\mathrm{c},i-1}}^{+}\mathbf{Q}_{i-1}^{+}(i) + \boldsymbol{\Phi}_{q_{\mathrm{c},i-1}}^{-}\mathbf{Q}_{i-1}^{-}(i)\right) - \left(\boldsymbol{\Phi}_{q_{\mathrm{c},i}}^{+}\mathbf{Q}_{i}^{+}(i) + \boldsymbol{\Phi}_{q_{\mathrm{c},i}}^{-}\mathbf{Q}_{i}^{-}(i)\right) = \mathbf{0} \tag{37}$$

and the continuity of the normal loads at the interface is written by:

$$\left(\boldsymbol{\Phi}_{F_{i-1}}^{+}\mathbf{Q}_{i-1}^{+}(i) + \boldsymbol{\Phi}_{F_{i-1}}^{-}\mathbf{Q}_{i-1}^{-}(i)\right) + \left(\boldsymbol{\Phi}_{F_{i}}^{+}\mathbf{Q}_{i}^{+}(i) + \boldsymbol{\Phi}_{F_{i}}^{-}\mathbf{Q}_{i}^{-}(i)\right) = \mathbf{0} \tag{38}$$

For example, in the case of the problem of the transmission of sound through an interface composed by 2 poroelastic layers made in different materials, the wave modes in the two domains are respectively given by $(\boldsymbol{\Phi}_1, \boldsymbol{\mu}_1)$ and $(\boldsymbol{\Phi}_2, \boldsymbol{\mu}_2)$, with $\|\boldsymbol{\mu}_1\| < 1$ and $\|\boldsymbol{\mu}_2\| < 1$. The correction matrix $\mathbf{D}_{\text{corr}}$ is then given by Eq. (33) using the following expressions:

$$\mathbf{B} = \begin{bmatrix} \mathbf{I} & (\boldsymbol{\Phi}_{F_1}^{+})^{-1}\boldsymbol{\Phi}_{F_1}^{-}\boldsymbol{\mu}_1 & \mathbf{0} & \mathbf{0} \\ (\boldsymbol{\Phi}_{q_{\mathrm{c},1}}^{-})^{-1}\boldsymbol{\Phi}_{q_{\mathrm{c},1}}^{+}\boldsymbol{\mu}_1 & \mathbf{I} & -(\boldsymbol{\Phi}_{q_{\mathrm{c},1}}^{-})^{-1}\boldsymbol{\Phi}_{q_{\mathrm{c},2}}^{+} & -(\boldsymbol{\Phi}_{q_{\mathrm{c},1}}^{-})^{-1}\boldsymbol{\Phi}_{q_{\mathrm{c},2}}^{-}\boldsymbol{\mu}_2 \\ (\boldsymbol{\Phi}_{F_2}^{+})^{-1}\boldsymbol{\Phi}_{F_1}^{+}\boldsymbol{\mu}_1 & (\boldsymbol{\Phi}_{F_2}^{+})^{-1}\boldsymbol{\Phi}_{F_1}^{-} & \mathbf{I} & (\boldsymbol{\Phi}_{F_2}^{+})^{-1}\boldsymbol{\Phi}_{F_2}^{-}\boldsymbol{\mu}_2 \\ \mathbf{0} & \mathbf{0} & (\boldsymbol{\Phi}_{F_2}^{-})^{-1}\boldsymbol{\Phi}_{F_2}^{+}\boldsymbol{\mu}_2 & \mathbf{I} \end{bmatrix}, \tag{39}$$

$$\mathbf{C} = \begin{bmatrix} \left(\boldsymbol{\Phi}_{F_1}^{+}\right)^{-1}\mathbf{D}_{\mathrm{P1}} & \mathbf{0} \\ \mathbf{0} & \mathbf{0} \\ \mathbf{0} & \mathbf{0} \\ \mathbf{0} & -\left(\boldsymbol{\Phi}_{F_2}^{-}\right)^{-1}\mathbf{D}_{\mathrm{P2}} \end{bmatrix} \quad \text{and} \quad \mathbf{I}_1 = \begin{bmatrix} \mathbf{I} & \mathbf{0} & \mathbf{0} & \mathbf{0} \\ \mathbf{0} & \boldsymbol{\mu}_1 & \mathbf{0} & \mathbf{0} \end{bmatrix}, \quad \mathbf{I}_2 = \begin{bmatrix} \mathbf{0} & \mathbf{0} & \boldsymbol{\mu}_2 & \mathbf{0} \\ \mathbf{0} & \mathbf{0} & \mathbf{0} & \mathbf{I} \end{bmatrix}. \tag{40}$$

3 Numerical examples

In this section we present two numerical examples validating the present approach, in the case of an absorption problem and a transmission problem, in the case of single and bilayer samples. It is shown in particular that, at the difference of impedance approach or hybrid FE-TMM algorithms[7], the present approach makes possible to take into account the effects of the lateral boundary conditions applied on the sample. If they can be neglected in the case of samples of large area, they can modify strongly the acoustic behaviour of the sample when small dimensions are considered, depending on the material. The parameters of the materials are provided in Appendix A in Table 1.

3.1 Absorption case

We consider here a rectangular acoustic cavity of dimensions $L_x = 40\mathrm{cm}$, $L_y = 30\mathrm{cm}$ and $L_z = 50\mathrm{cm}$, excited by an imposed displacement in the corner $(x = 0, y = 0, z = L_z)$. In this cavity, a poroelastic

layer of thickness $L_{\mathrm{P}} = 5\mathrm{cm}$ of material A is glued on the wall $z = 0$ (see Fig. 2). The mesh consists in $(15 \times 10 \times 25)$ linear hexaedric H8 elements for the acoustic domain and $(15 \times 10 \times 5)$ H8 elements for the poroelastic domain. Because the absorbing layer is very soft and bonded on a hard wall, the poroelastic layer is modelled by a fluid with limp frame assumption. It is furthermore justified by the Frame Stiffness Influence [21] of the material ($FSI < 0.5$).

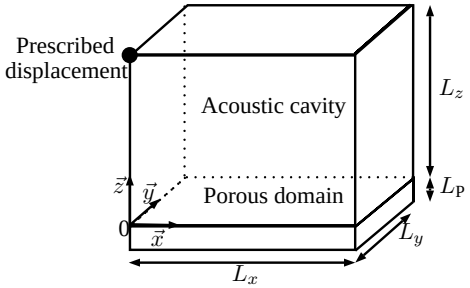

Figure 2: Description and notation for the absorption problem.

Figure 3 shows the sound pressure level in the cavity predicted with FEM, present approach and normal impedance. The sound pressure levels predicted by the three approaches are well superposed on the whole frequency range.

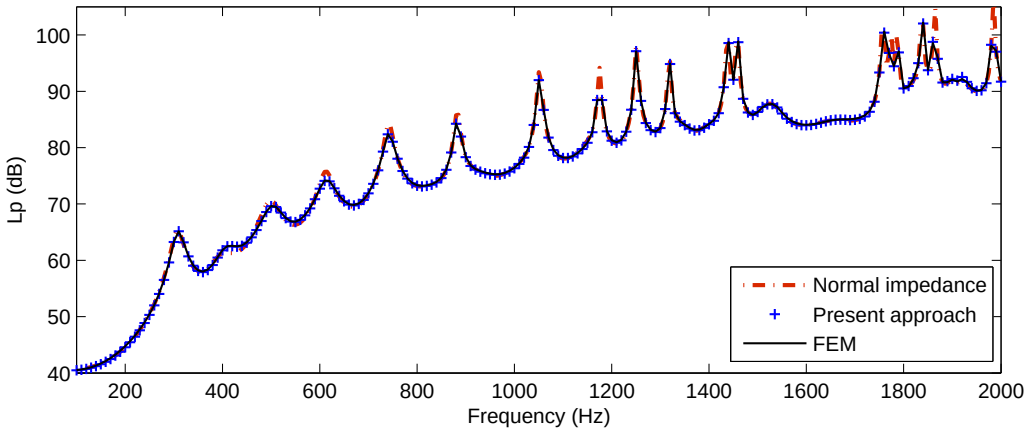

Figure 3: Sound pressure level in the acoustic cavity.

3.2 Transmission case

We consider here a transmission tube of rectangular section $L_x = 10\mathrm{cm}$ and $L_y = 8\mathrm{cm}$. The length of the two acoustic cavities are $L_e = L_r = 45\mathrm{cm}$. All of the walls are rigid. Between these two cavities is placed a dissipative interface composed of $L_1 = 5\mathrm{cm}$ of material A and $L_2 = 3\mathrm{cm}$ of material B. The excitation room is excited by an imposed acoustic displacement in the corner $(x, y, z) = (0, 0, 0)$, and all other walls are considered as rigid. The boundary conditions at the lateral faces of the poroelastic samples are set either sliding or clamped for each of the materials.

Figure 5 presents the sound pressure levels in each cavity when using Finite Elements or condensation procedure, in the case of sliding or clamped boundary conditions on the lateral walls of the muffler. It can be observed that the results of FEM are superposed with the results obtained with the present approach for each type of lateral boundary conditions. However, due to infinite geometry assumption made in TMM, the coupled FEM-TMM presented in [7] can only be applied in the case of sliding boundary conditions. In this case, the results are superposed with FEM.

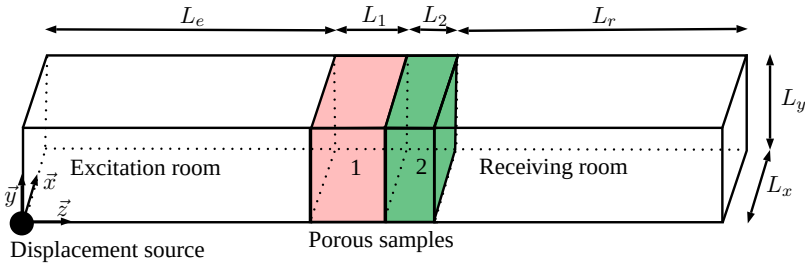

Figure 4: Description and notation for the transmission problem.

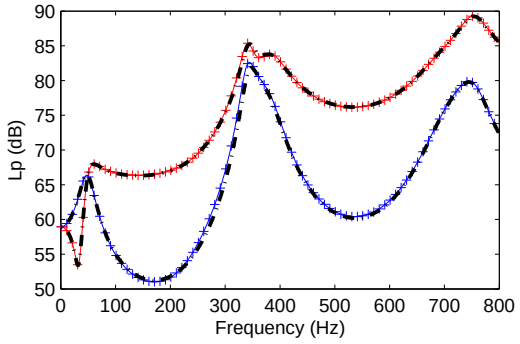

(a) Sliding boundary condition. line: FEM, + present, dash-dots: FEM+TMM.

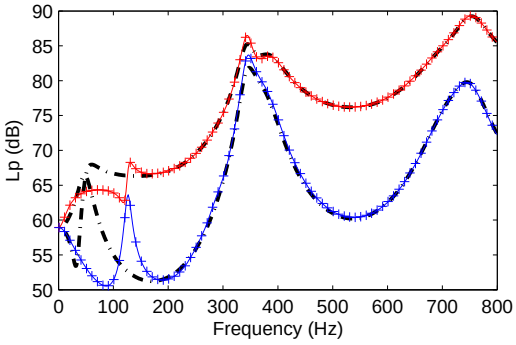

(b) Clamped boundary condition. line: FEM, + present, dash-dots: sliding boundary condition.

Figure 5: Sound pressure levels in excitation between 1Hz and 800Hz. Red: emission room and blue: reception room.

For higher frequencies, section modes of the acoustic tube becomes propagative, resulting in a non-uniform excitation pressure field in both cavities. The present approach leads once again to the same results as Finite Elements. In this case, $(8 \times 8 \times 60)$ linear H8 elements have been used for each cavity, leading to at least 10 acoustic wavelengths per element. In the thickness direction of the two poroelastic domains, 20 and 15 elements are used in the FEM study.

A good agreement can be observed between the two curves in the whole frequency range. A slight difference occurs in the high frequency range, making possible to illustrate an advantage of the method over FEM. In fact, the result of the condensation procedure does not depend on the number of elements in the thickness, at the difference of FEM, for which the number of elements in thickness is a discriminating parameter, especially for problem involving compression of materials. The slight difference is actually due to the non convergence of FEM: the very small wavelengths travelling in the materials at such frequencies need a mesh much finer to reach convergence at these frequencies.

4 Remarks on computation times

The gain achieved with this method grows with the ratio of the thickness dimension by the section area. This gain is illustrated on Fig. 7. Because computation times observed with our in-house code are not representative of times obtained with modern finite element software, we present here times divided by an arbitrary reference value. This value was fixed equal to the time needed to solve the problem with the present approach in the case of the finest section mesh (100 dofs in the section).

It can be observed that the time needed to compute the section modes increases with the size of the section mesh, as well as the time needed to compute the correction matrix $\mathbf{D}_{\text{corr}}$. This calculation involves solving a linear system of larger size, in which inverse matrices are needed for conditioning. On the other hand, it is

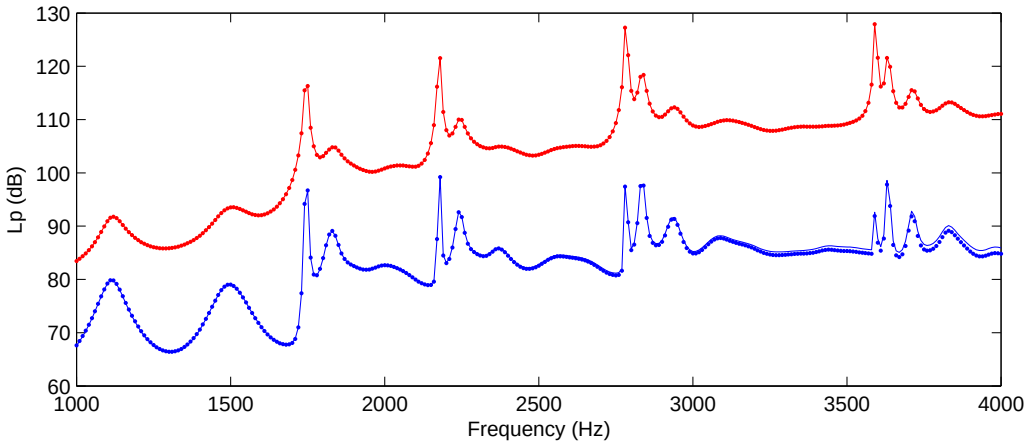

Figure 6: Pressure levels in the higher frequency range. Red: Emission room, blue: reception room. line: FEM, dots: present approach.

clear on Fig. 7 that the time needed to solve the problem does not depend on the number of elements used to discretize the thickness direction. If all of the modes are taken, the number of unknowns associated to each interface component is equal to twice the number of dofs in one section. This aspect is interesting in two cases: (i) when a large number of elements are used in the thickness, (ii) or when several iterations are needed to evaluate the sound pressure level depending on the thickness of the multilayer and on the order in which the materials are placed.

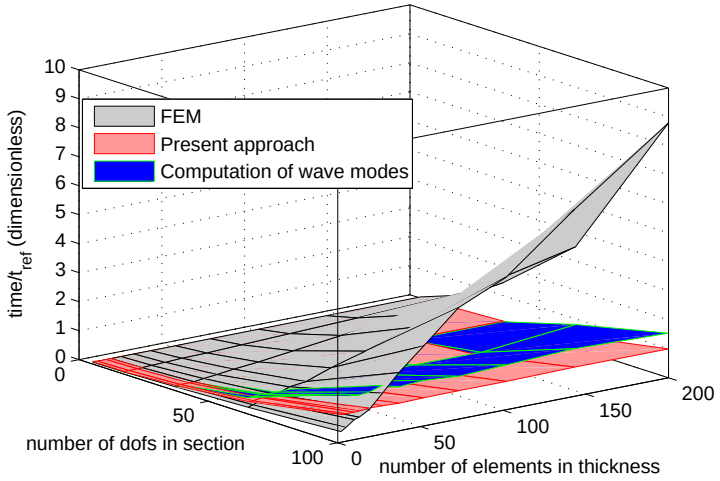

Figure 7: Relative computation times obtained for the absorption problem with 10 acoustic elements along z direction, depending on the number of dofs in the section, the number of elements in thickness and the method.

Several strategies can be adopted to reduce further the computational cost. First, component mode synthesis can be used on the acoustic domain to reduce the number of dofs associated to it. In [3] was shown that a limit of the method lies in the number of dofs associated to the poroelastic domain: its efficiency is larger when the number of acoustic dofs is much larger than the number of dofs associated to dissipative interface. With the present approach, all of the poroelastic unknowns are condensed, so that CMS techniques may be very efficient. On another hand, the method can be easily coupled with an approach using Padé approximants (see for example [4]). Thus, the number of frequencies in which the modes are computed would be reduced to a small number of evaluation frequencies, saving large computation times and memory, while time needed to

predict the sound level at these frequencies would be reduced by using a condensed model (present approach) instead of FEM. Finally, a point still under investigation is the question of the use of all of the waves to predict the response.

5 Conclusion

A procedure to condense the unknowns associated to dissipative domains has been presented. The main idea lies in the use of propagative waves in the thickness direction to compute the load exerted by the interface on the acoustic part, as a function of the ambient pressure. Thus, the algorithm results in a system of lower size than the original system. The method applies to flat interfaces, and can be considered as an generalized impedance model for the dissipative interfaces, because it does not assume any hypothesis on the displacement and stress fields in the section plane of the dissipative interface. Thus lateral boundary conditions exerted on the interface can be taken into account as well as non localized effects. Finally, the projection of the displacement field and of the normal load fields on the progressive waves makes possible to reach convergence of the results at any frequency with only 1 element in the thickness direction, making possible to save computational cost in the case of thick layers.

Acknowledgements

The research presented in this paper was performed within the framework of the LABEX CELYA ("Centre Lyonnais d'Acoustique", ANR-10-LABX-0060) of Université de Lyon, and funded by a doctoral grant of the French Ministry of Higher Education and Research.

References

[1] O. Dazel, B. Brouard, J-P. Groby, and P. Göransson, *A normal modes technique to reduce the order of poroelastic models: application to 2D and coupled 3D models*, International Journal for Numerical Methods in Engineering, Vol. 95, No. 2, John Wiley & Sons (2013), pp. 110-128.

[2] R. Rumpler, J-F. Deü, and P. Göransson, *A modal-based reduction method for sound absorbing porous materials in poro-acoustic finite element models*, The Journal of the Acoustical Society of America, Vol. 132, No. 5, ASA (2012), pp. 3162-3179.

[3] R. Rumpler, A. Legay, and J-F. Deü, *Performance of a restrained-interface substructuring FE model for reduction of structural-acoustic problems with poroelastic damping*, Computers & Structures, Vol. 89, No. 23, Elsevier (2011), pp. 2233-2248.

[4] R. Rumpler, P. Göransson, and J-F. Deü. *A finite element approach combining a reduced-order system, Padé approximants, and an adaptive frequency windowing for fast multi-frequency solution of poro-acoustic problems*, International Journal for Numerical Methods in Engineering, Vol. 97, No. 10, John Wiley & Sons (2014), pp. 759-784.

[5] J-D. Chazot, B. Nennig, and E. Perrey-Debain, *Harmonic response computation of poroelastic multi-layered structures using ZPST shell elements*, Computers & Structures, Vol. 121, Elsevier (2013), pp. 99-107.

[6] J-F. Allard and N. Atalla, *Propagation of Sound in Porous Media: Modelling Sound Absorbing Materials Second edition*, Wiley, New York (2009).

[7] F. Chevillotte and R. Panneton, *Coupling transfer matrix method to finite element method for analyzing the acoustics of complex hollow body networks*, Applied Acoustics, Vol. 72, No. 12, Elsevier (2011), pp. 962-968.

[8] L. Alimonti, N. Atalla, A. Berry, and F. Sgard, *Assessment of a hybrid finite element-transfer matrix model for flat structures with homogeneous acoustic treatments*. The Journal of the Acoustical Society of America, Vol. 135, No. 5, ASA (2014), pp. 2694-2705.

[9] W.X. Zhong and F.W. Williams, *On the direct solution of wave propagation for repetitive structures*, Journal of Sound and Vibration, Vol. 181, No. 3, Academic Press (1995), pp. 485-501.

[10] J-M. Mencik and M.N. Ichchou. *Multi-mode propagation and diffusion in structures through finite elements*, European Journal of Mechanics -A/Solids, Vol. 2, No. 5, Elsevier (2005), pp. 877-898.

[11] B.R. Mace, D. Duhamel, M.J. Brennan, and L. Hinke. *Finite element prediction of wave motion in structural waveguides*, The Journal of the Acoustical Society of America, Vol. 117, No. 5, ASA (2005), pp. 2835-2843.

[12] D. Chronopoulos, M.N. Ichchou, B. Troclet, and O. Bareille, *Computing the broadband vibroacoustic response of arbitrarily thick layered panels by a wave finite element approach*, Applied Acoustics, Vol. 77, Elsevier (2014), pp. 89-98.

[13] D. Chronopoulos, B. Troclet, M.N. Ichchou, and J-P. Lainé, *A unified approach for the broadband vibroacoustic response of composite shells*, Composites Part B: Engineering, Vol. 43, No. 4, Elsevier (2012), pp. 1837-1846.

[14] Y.Waki, B.R. Mace, and M.J. Brennan. *Numerical issues concerning the wave and finite element method for free and forced vibrations of waveguides*, Journal of Sound and Vibration, Vol. 327, No. 1, Elsevier (2009), pp. 92-108.

[15] M.N. Ichchou, J-M. Mencik, and W. Zhou. *Wave finite elements for low and mid-frequency description of coupled structures with damage*, Computer methods in applied mechanics and engineering, Vol. 198, No. 15, Elsevier (2009), pp. 1311-1326.

[16] M.N. Ichchou, F. Bouchoucha, M.A. Ben Souf, O. Dessombz, and M. Haddar. *Stochastic wave finite element for random periodic media through first-order perturbation*,Computer Methods in Applied Mechanics and Engineering, Vol. 200, No. 41, Elsevier (2011), pp. 2805-2813.

[17] M.N. Ichchou, S. Akrout, and J-M. Mencik. *Guided waves group and energy velocities via finite elements*. Journal of Sound and Vibration, Vol. 305, No. 4, Elsevier (2007), pp. 931-944.

[18] O. Dazel, B. Brouard, C. Depollier, and S. Griffiths, *An alternative Biot's displacement formulation for porous materials*, The Journal of the Acoustical Society of America, Vol. 121, No. 6, ASA (2007), pp. 3509-3516.

[19] C.-H. Jeong and Jonas Brunskog, *The equivalent incidence angle for porous absorbers backed by a hard surface*, The Journal of the Acoustical Society of America, Vol. 134, No. 6, ASA (2013), pp. 4590-4598.

[20] J-M. Mencik, *On the low-and mid-frequency forced response of elastic structures using wave finite elements with one-dimensional propagation*, Computers & Structures, Vol. 88, No. 11, Elsevier (2010), pp. 674-689.

[21] O. Doutres, N. Dauchez, J-M. Génevaux, and O. Dazel, *Validity of the limp model for porous materials: A criterion based on the Biot theory*, The Journal of the Acoustical Society of America, Vol. 122, No. 4, ASA (2007), pp. 2038-2048.

A Material parameters

Parameter	Material A	Material B
Acoustic parameters		
Porosity ϕ	0.937	0.9520
Resistivity σ $(\mathrm{N.s.m^{-4}})$	50485	21300
Tortuosity α_∞	2.57	1.6
Viscous length Λ $(\mu\mathrm{m})$	57.41	100
Thermal length Λ' $(\mu\mathrm{m})$	61.62	300
Structural parameters		
Skeleton density ρ_s $(\mathrm{kg.m^{-3}})$	95.66	38.4
First Lame's coefficient λ (Pa)	57037	34420
Second Lame's coefficient μ (Pa)	24444	10870
Hysteretic dissipation η	0.105	0.04

Table 1: Parameters of materials.